Analysis and Design of Class E Power Amplifier with Finite DC-Feed Inductance and Series Inductance Network

Chuicai Rong [1,2], Xiansuo Liu [1], Yuehang Xu [1]*, Ruimin Xu [1], and Mingyao Xia [1]

[1] School of Electronic Engineering
University of Electronic Science and Technology of China, Chengdu, 611731, China
*yuehangxu@uestc.edu.cn

[2] School of Physics and Electronic Information
Gannan Normal University, Ganzhou, Jiangxi, 341000, China
chuicair@126.com

Abstract ─ With the increasing operation frequency, it is essential to take into account the parasitic parameters of transistor for high efficiency microwave power amplifier design. In this paper, a class E power amplifier with finite dc-feed inductance and series inductance network is analyzed including the parasitic inductance of transistor. The analytical design expressions are derived. And the effects of series inductance on the load network parameter are obtained. The results suggest that this new topology can be used in broadband power amplifiers design by making full use of transistor's output parasitic inductance. A GaN HEMT power amplifier is designed with the proposed topology for validation purpose. Experimental results show that the amplifier can realize from 2.5 GHz to 3.5 GHz (33.3％) with measured drain efficiency larger than 60% and output power larger than 34 dBm. The measured performance shows good agreement with the theoretical performance predicted by the equations.

Index Terms ─ Broadband, class E power amplifier, finite dc-feed inductance, parasitic inductance.

I. INTRODUCTION

One of the most important features of RF power amplifier (PA) is power efficiency. By increasing the efficiency, PA will consume less supply power and requires less heat sinking. This allows a reduction of battery size and an increase in battery life. The switch mode class E PA [1] is a good candidate for high efficiency PA due to its design simplicity.

The class E PA with finite dc-feed inductance [2, 3] is one important topology of the class E PA. It has smaller inductance than the RF-choke and thus has lower loss [4] due to a smaller electrical series resistance (ESR). It can obtain greater power capability than other class E topology. And the larger load resistance makes the design of the matching network easier. These advantages make this topology widely attracted. In [5], the effects of dc-feed inductance, the quality factor (Q_L) of the series-tuned circuit, and the switching-device on resistance have been analyzed. In [6], the maximum frequency of the class E PA with finite dc-feed inductance is discussed. In [7], an arbitrary duty-cycle and finite dc-feed inductance is discussed. In [8], the power dissipation in each component is calculated. In [9], load transformation networks for wideband operation is investigated. In [10], the analytical expression of the switch peak voltage is presented. With the increasing operation frequency, it is essential to take into account all the device parasitic parameters [11, 12]. In [13, 14], the normalized optimum load network parameters versus normalized bond-wire inductance for parallel-circuit class E PA are presented. But the parallel-circuit class E PA is only one kind of the class E power amplifier with finite dc-feed inductance. To get the general results, it is necessary to further study the effect of the device output series inductance on the load network parameters of the class E power amplifier with finite dc-feed inductance.

In this paper, a theoretical description of the class E PA with finite dc-feed inductance and series inductance network is presented. The analysis takes into account the transistor's output parasitic inductance on the load network parameters of the class E PA with finite dc-feed inductance. Thus, the analysis can provide useful and accurate design to the class E PA in higher operation frequency. Finally, a design case is constructed in the laboratory in order to verify the theoretical predictions for demonstration purpose.

II. CIRCUIT DESCRIPTION

The class E power amplifier with finite dc-feed inductance and series inductance is shown in the Fig. 1. The load network consists of the shunt capacitance C_0, a series inductance L_{series}, a parallel inductance L_0, a

series reactive element jX, and a load R. The shunt capacitance C_0 represents the intrinsic device output capacitance. The series inductance L_{series} can be considered as an adjustment parameter which include the bond-wire inductance and lead inductance. A parallel inductance L_0 represents the finite DC-feed inductance and the series reactive element jX can be positive (inductance) or negative (capacitance) or zero. The active device is considered to be an ideal switch.
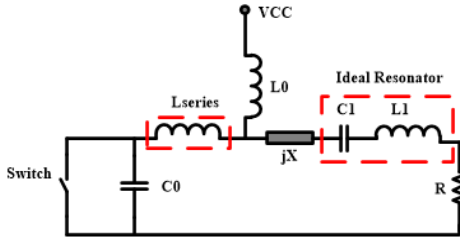

Fig. 1. Circuit of the class E power amplifier with finite dc-feed inductance and series inductance network.

To simplify analysis of the class E power amplifier with finite dc-feed inductance and series inductance, several assumptions are introduced in [13, 14]. For an idealized theoretical analysis, the moments of the switch-on is $\omega t = 0$ and switch-off is $\omega t = \pi$ with period of repeatability of the input driving signal $T = 2\pi$. Nominal conditions for voltage across the switch prior to the start of switch–on at the moment $\omega t = 2\pi$ are:

$$v(\omega t)\big|_{\omega t = 2\pi} = 0, \tag{1}$$

$$\frac{dv(\omega t)}{dt}\bigg|_{\omega t = 2\pi} = 0. \tag{2}$$

The output current flowing through the load R is written as sinusoidal by:

$$i_R(\omega t) = I_R \sin(\omega t + \phi), \tag{3}$$

where I_R is the load current amplitude and ϕ is the initial phase shift.

When the switch is turned on for $0 \le \omega t \le \pi$, the voltage on the switch is zero. The current flowing through the switch can be written as:

$$i(\omega t) = \frac{V_{cc}}{\omega L_0 (1+\alpha)} \omega t + \frac{\omega L_0 I_R}{\omega L_0 (1+\alpha)} \left[\sin(\omega t + \phi) - \sin\phi\right], \tag{4}$$

where $\alpha = L_{series}/L_0$.

When switch is off for $\pi \le \omega t \le 2\pi$, the current $i(\omega t) = 0$ and the current $i_{C_0}(\omega t) = i_{L_0}(\omega t) + i_R(\omega t)$ flowing the capacitance C_0 can be rewritten as:

$$\omega C_0 \frac{dv(\omega t)}{d(\omega t)} = \frac{1}{\omega L_0} \int_\pi^{\omega t} \left[V_{cc} - v(\omega t) - v_{L_{series}}(\omega t)\right] d(\omega t) + i_{L_0}(\pi) + I_R \sin(\omega t + \phi). \tag{5}$$

Differentiating both sides of (5), the second-order differential equation becomes:

$$\omega^2 C_0 L_0 (1+\alpha) \frac{d^2 v(\omega t)}{d(\omega t)^2} + v(\omega t) - V_{cc} - \omega L_0 I_R \cos(\omega t + \phi) = 0. \tag{6}$$

Under the initial off-state conditions,

$$v(\pi) = 0, \tag{7}$$

The current $i_{L_0}(\pi)$ flowing through the finite inductance L_0 is:

$$i_{L_0}(\pi) = \frac{V_{cc}\pi}{\omega L_0 (1+\alpha)} - \frac{1-\alpha}{1+\alpha} I_R \sin\phi. \tag{8}$$

The current flowing through the capacitance C_0 is:

$$i_{C_0}(\pi) = i_{L_0}(\pi) + i_R(\pi) = \frac{V_{cc}\pi - 2\omega L_0 I_R \sin\phi}{\omega L_0 (1+\alpha)}, \tag{9}$$

$$i_{C_0}(\omega t) = \omega C_0 \frac{dv(\omega t)}{d(\omega t)}, \tag{10}$$

$$\frac{dv(\omega t)}{d(\omega t)}\bigg|_{\omega t = \pi} = \frac{V_{cc}\pi - 2\omega L_0 I_R \sin\phi}{\omega^2 C_0 L_0 (1+\alpha)} = \frac{V_{cc}(\pi - 2p\sin\phi)}{Q^2}, \tag{11}$$

where

$$Q^2 = \omega^2 C_0 L_0 (1+\alpha) = \frac{\omega^2}{\omega_0^2}(1+\alpha) = \chi^2(1+\alpha), \tag{12}$$

$$\omega_0 = \frac{1}{\sqrt{C_0 L_0}}, \chi = \frac{\omega}{\omega_0}, p = \frac{\omega L_0 I_R}{V_{cc}}, \tag{13}$$

where χ is the normalized frequency. With the initial off-state conditions (7) and (11), the general solution of (6) can be obtained in the normalized forms:

$$\frac{v(\omega t)}{V_{cc}} = C_1 \cos(\frac{\omega t}{Q}) + C_2 \sin(\frac{\omega t}{Q}) + 1 - \frac{p}{Q^2 - 1}\cos(\omega t + \phi), \tag{14}$$

$$C_1 = -\left[\cos(\frac{\pi}{Q}) + \frac{\pi}{Q}\sin(\frac{\pi}{Q})\right] - \frac{Qp}{Q^2 - 1}\left[\frac{\cos\phi}{Q}\cos(\frac{\pi}{Q}) - \frac{Q^2 - 2}{Q^2}\sin\phi\sin(\frac{\pi}{Q})\right], \tag{15}$$

$$C_2 = \left[\frac{\pi}{Q}\cos(\frac{\pi}{Q}) - \sin(\frac{\pi}{Q})\right] - \frac{Qp}{Q^2 - 1}\left[\frac{\cos\phi}{Q}\sin(\frac{\pi}{Q}) - \frac{Q^2 - 2}{Q^2}\sin\phi\cos(\frac{\pi}{Q})\right]. \tag{16}$$

Applying nominal conditions of (1) and (2), the optimum parameters ϕ and p as functions of Q are:

$$\tan\phi = -\frac{\pi + \pi\cos(\frac{\pi}{Q}) + 2Q\sin(\frac{\pi}{Q})}{2(Q^2 - 1)\left[1 - \cos(\frac{\pi}{Q})\right] + Q\pi\sin(\frac{\pi}{Q})}, \tag{17}$$

$$p = \frac{(1-Q^2)\left[Q\sin(\frac{\pi}{Q}) + \pi\cos(\frac{\pi}{Q})\right]}{Q\cos\phi\sin(\frac{\pi}{Q}) + \left[Q^2 + (2-Q^2)\cos(\frac{\pi}{Q})\right]\sin\phi}, \quad (18)$$

where Q is a function of α and χ. Figure 2 shows the initial phase shift ϕ versus α and χ. With the increasing of χ, the initial phase shift ϕ decreases. With the increasing of α, the initial phase shift ϕ decreases and the gradient of the initial phase shift ϕ is slow in broadband. Thus, it is easy to match for load network.
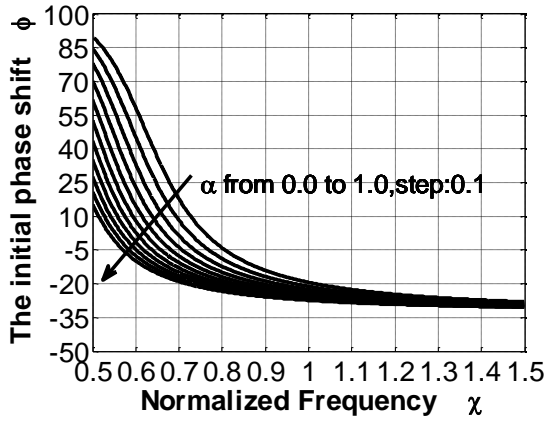

Fig. 2. Initial phase shift ϕ versus α and χ.

The normalized load-network parameters inductance L_0, capacitance C_0, and resistance R are presented as functions of parameters p, ϕ, α, Q, as below:

$$\frac{\omega L_0}{R} = \frac{p(1+\alpha)}{\frac{\pi}{2p} + \frac{2\cos\phi}{\pi} - \sin\phi}, \quad (19)$$

$$\omega C_0 R = \frac{Q^2}{p(1+\alpha)^2}\left[\frac{\pi}{2p} + \frac{2\cos\phi}{\pi} - \sin\phi\right], \quad (20)$$

$$\frac{RP_{out}}{V_{cc}^2} = \frac{\left[\frac{\pi^2}{2p} + 2\cos\phi - \pi\sin\phi\right]^2}{2\pi^2(1+\alpha)^2}. \quad (21)$$

From the viewpoint of mathematics, they are only functions of parameters α and χ. Figure 3 shows the parameter $\omega L_0/R$ versus α and χ. With the increasing of χ, the parameter $\omega L_0/R$ increases. With the increasing of α, the parameter $\omega L_0/R$ increases.

Figure 4 shows the parameter $\omega C_0 R$ versus α and χ. The parameter $\omega C_0 R$ has maximum of 0.7021 when $\chi = 0.681$ and $\alpha = 0$. Then the maximum frequency of the class E power amplifier with finite dc-feed inductance

and series inductance is $f_{max} = 0.7021/(2\pi C_0 R)$. With the increasing of α, the parameter $\omega C_0 R$ decreases.
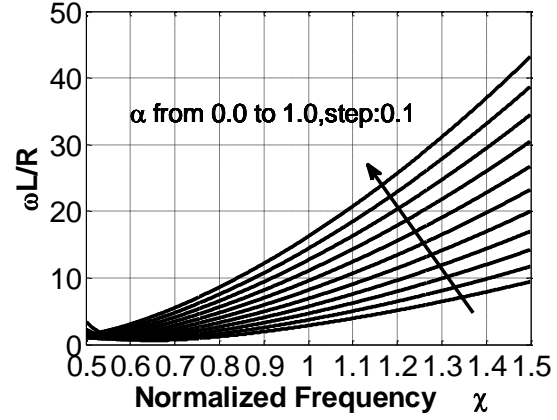

Fig. 3. $\omega L_0/R$ versus α and χ.

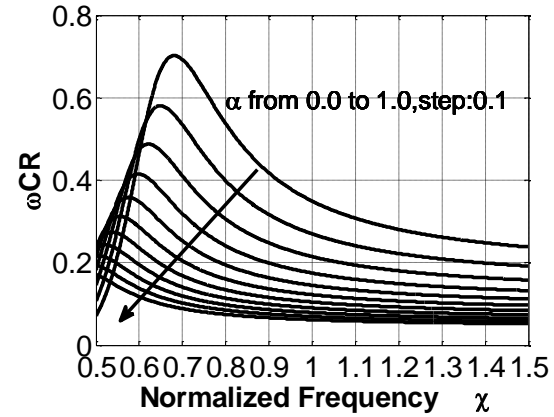
Fig. 4. $\omega C_0 R$ versus α and χ.

Figure 5 shows the parameter RP_{out}/V_{cc}^2 versus α and χ. The parameter RP_{out}/V_{cc}^2 has maximum of 1.3633 when $\chi = 0.709$ and $\alpha = 0$. Then the maximum load resistance of the class E power amplifier with finite dc-feed inductance and series inductance is $R_{max} = 1.3633V_{cc}^2/P_{out}$. With the increasing of α, the parameter RP_{out}/V_{cc}^2 decreases.

The Equations (22) through (25) below present the analytical expressions of the voltage across the reactance X. The Equations (26) through (29) below present the analytical expressions of the voltage across the resistance R.

$$V_X = \frac{1}{\pi}(V_{X1} + V_{X2} + V_{X3}), \quad (22)$$

$$V_{X1} = \frac{\alpha(\frac{\pi p}{2} - 2\sin\phi)}{1+\alpha} + \frac{\pi p(\alpha\chi^2 - 1)}{2(Q^2 - 1)} + 2\sin\phi, \quad (23)$$

$$V_{X2} = \frac{C_1}{2}\left(1 - \frac{\alpha\chi^2}{Q^2}\right)\left\{\begin{array}{l}\frac{Q}{1+Q}\left[\sin\left(\frac{2\pi}{Q}+\phi\right)+\sin\left(\frac{\pi}{Q}+\phi\right)\right]\\+\frac{Q}{1-Q}\left[\sin\left(\frac{2\pi}{Q}-\phi\right)+\sin\left(\frac{\pi}{Q}-\phi\right)\right]\end{array}\right\},$$

(24)

$$V_{X3} = -\frac{C_2}{2}\left(1 - \frac{\alpha\chi^2}{Q^2}\right)\left\{\begin{array}{l}\frac{Q}{1+Q}\left[\cos\left(\frac{2\pi}{Q}+\phi\right)+\cos\left(\frac{\pi}{Q}+\phi\right)\right]\\+\frac{Q}{1-Q}\left[\cos\left(\frac{2\pi}{Q}-\phi\right)+\cos\left(\frac{\pi}{Q}-\phi\right)\right]\end{array}\right\},$$

(25)

$$V_R = \frac{1}{\pi}\left(V_{R1}+V_{R2}+V_{R3}\right), \qquad (26)$$

$$V_{R1} = -\frac{2\cos\phi}{1+\alpha}, \qquad (27)$$

$$V_{R2} = \frac{C_1}{2}\left(1 - \frac{\alpha\chi^2}{Q^2}\right)\left\{\begin{array}{l}\frac{Q}{1-Q}\left[\cos\left(\frac{2\pi}{Q}-\phi\right)+\cos\left(\frac{\pi}{Q}-\phi\right)\right]\\-\frac{Q}{1+Q}\left[\cos\left(\frac{2\pi}{Q}+\phi\right)+\cos\left(\frac{\pi}{Q}+\phi\right)\right]\end{array}\right\},$$

(28)

$$V_{R3} = -\frac{C_2}{2}\left(1 - \frac{\alpha\chi^2}{Q^2}\right)\left\{\begin{array}{l}\frac{Q}{1+Q}\left[\sin\left(\frac{2\pi}{Q}+\phi\right)+\sin\left(\frac{\pi}{Q}+\phi\right)\right]\\-\frac{Q}{1-Q}\left[\sin\left(\frac{2\pi}{Q}-\phi\right)+\sin\left(\frac{\pi}{Q}-\phi\right)\right]\end{array}\right\},$$
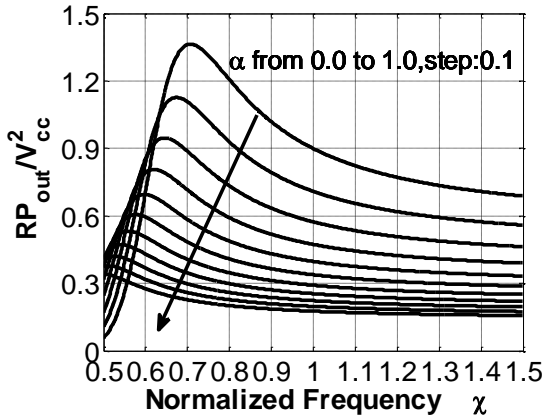
(29)

$$\frac{X}{R} = \frac{V_X}{V_R}. \qquad (30)$$

Fig. 5. RP_{out}/V_{cc}^2 versus α and χ.

Figure 6 shows the parameter X/R versus α and χ. The X/R is equal to zero when $\chi < 0.708$ and $\alpha = 0$, which is the parallel-circuit class E PA. When $\chi < 0.708$ and $\alpha = 0$, the reactance X is positive (inductive reactance). When $\chi < 0.708$ and $\alpha = 0$, the reactance X is negative (capacitive reactance). When $\chi < 0.708$, with the increasing of α, the parameter X/R decreases, even below zero. When $\chi < 0.708$, with the increasing of α, the parameter X/R increases.

In Table 1, the optimized load-network parameters of the different class E modes include class E with shunt filter and the class E with finite dc-feed inductance and series inductance are shown in a normalized form. As can be seen, the class E with finite dc-feed inductance and series inductance offers the larger value of the power output capability c_P and the load R, which is 3.18 times higher than that for class E with shunt capacitance.
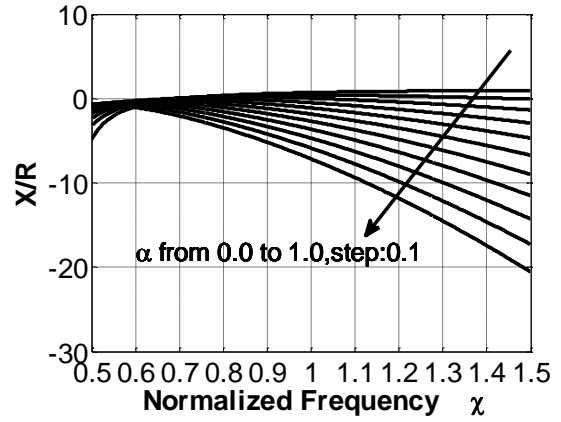

Fig. 6. X/R versus α and χ.

Table 1: Load network parameters for different class E modes

Normalized Load-Network Parameter	Class E with Shunt Capacitance and Shunt Filter[15]	Class E with Finite DC-Feed Inductance and Series Inductance
$\frac{X}{R}$	1.4836	0 ($\alpha = 0$, $\chi = 0.708$)
ωCR	0.261	0.7021 ($\alpha = 0$, $\chi = 0.681$)
$\frac{P_{out}R}{V_{CC}^2}$	0.4281	1.3633 ($\alpha = 0$, $\chi = 0.681$)
$\frac{f_{max}C_{out}V_{CC}^2}{P_{out}}$	0.097	0.1505 ($\alpha = 0$, $\chi = 0.693$)
c_P	0.09825	0.1049 ($\alpha = 0$, $\chi = 0.6689$)

III. DESIGN CONSIDERATION

For broadband PA design [15], the susceptance of the network is an important parameter. Figure 7 shows the susceptance $Imag[V_{cc}^2 Y_{net}(\chi)/P_{out}]$ of the class E PA with finite dc-feed inductance and series inductance.

The χ when α increase from 0.0 to 1.0 by step 0.1. When $\alpha = 0$, the difference of susceptance is 0.2389 in the frequency range $(0.5 \leq \chi \leq 1.5)$. When $\alpha = 1$, the difference of susceptance is 0.0381 in the frequency range $(0.5 \leq \chi \leq 1.5)$. The parameter α can be used to control the difference of susceptance over a wide frequency range.
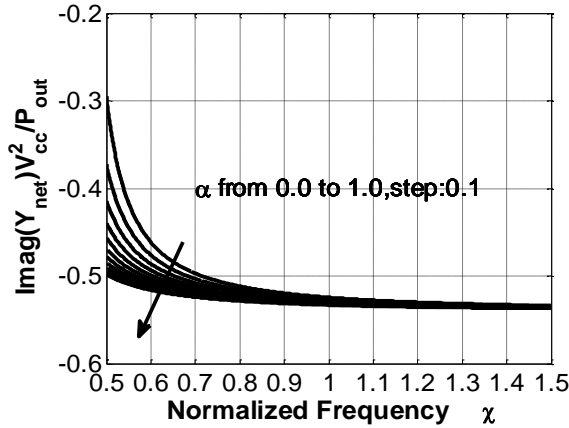

Fig. 7. Susceptance $Imag[V_{cc}^2 Y_{net}(\chi)/P_{out}]$ versus α and χ.

Figure 8 shows the conductance $\mathrm{Re}\,al[V_{cc}^2 Y_{net}(\chi)/P_{out}]$ of class E PA with finite dc-feed inductance and series inductance versus χ when α increase from 0.0 to 1.0 by step 0.1. When $\alpha = 0$, the difference of conductance is 0.0239 in the frequency range $(0.5 \leq \chi \leq 1.5)$. When $\alpha = 1$, the difference of conductance is 0.01 in the frequency range $(0.5 \leq \chi \leq 1.5)$. The parameter α can be used to control the difference of conductance over a wide frequency range.
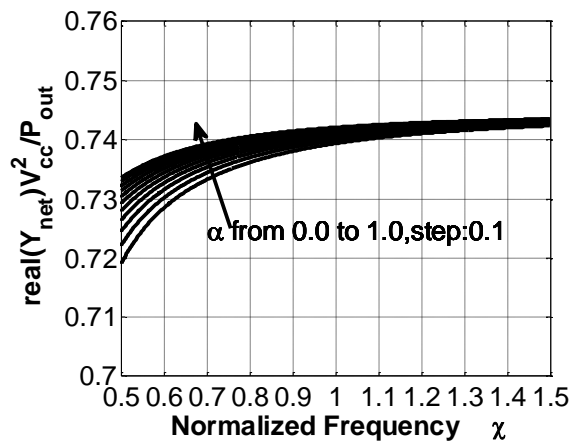

Fig. 8. Conductance $\mathrm{Re}\,al[V_{cc}^2 Y_{net}(\chi)/P_{out}]$ versus α and χ.

Figure 9 shows load phase angle of class E PA with finite dc-feed inductance and series inductance versus χ when α increase from 0.0 to 1.0 by step 0.1. When $\alpha = 0$, the difference of load phase angle is 13.42^o in the frequency range $(0.5 \leq \chi \leq 1.5)$. When $\alpha = 1$, the difference of load phase angle is 1.65^o in the frequency range $(0.5 \leq \chi \leq 1.5)$. The parameter α can be used to control the difference of load phase angle over a wide frequency range.

In a word, by proper choice of the series inductance αL_0, which produces a zero total variation of the susceptance, the conductance and the load phase angle are controllable over a wide frequency range.
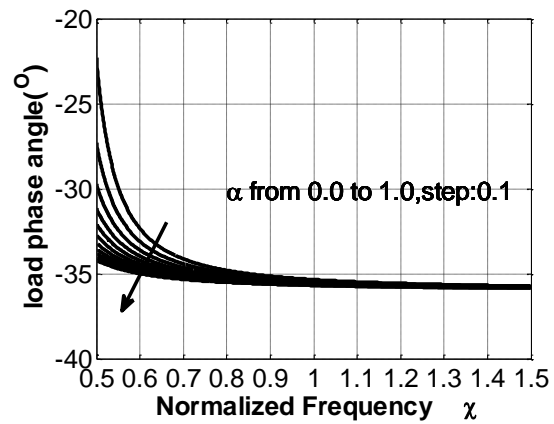

Fig. 9. Load phase angle versus α and χ.

IV. SIMULATION AND IMPLEMENTATION

A complete circuit schematic of class E PA with finite dc-feed inductance and series inductance is shown in Fig. 10. A 0.25μm gate length GaN HEMT with 1.25 mm total gate-width $(C_{ds} = 0.254 pF)$ is used to design a Class E PA with finite dc-feed inductance and series inductance. The simulation of amplifier is realized by combing Ansys HFSS and Keysight ADS. The HFSS is used to simulate passive part of matching network. A large signal model is established to simulate the large signal performance of amplifier with HB simulation tool [16]. The total inductance $L_{series} = L_{para} + L_{wire} + L_1$, where L_{para} is the output parasitic inductance of transistor, L_{wire} is the inductance induced by bonding wire for hybrid amplifier, and L_1 is the adjustive inductance. The parasitic output capacitance C_{out} of the transistor, L_{series}, L_2, and the reactance C_3 constitute the double L-type network. The inductance L_1 and L_2 is realized by the high impedance transmission line.

Typically, class E PA achieve high efficiency when the output power gain at 3 dB or 4 dB compression point

[17, 18]. So it is necessary to suppress the second and third harmonic to improve efficiency. Low pass match was used in operation frequency and suppress the harmonics both in the input and output network [19, 20]. Shunt resistance R_1 and capacitance C_2 in the input network was used to improve the low frequency stability. The photo of the class E PA with finite dc-feed inductance and series inductance is shown in Fig. 11.
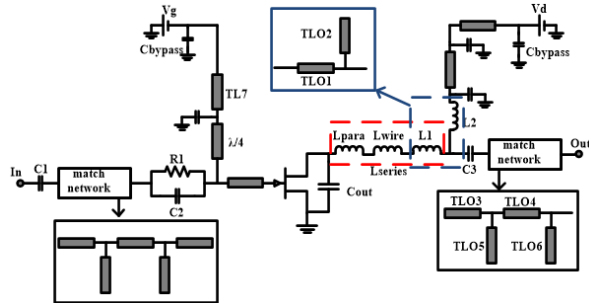

Fig. 10. The circuit schematic of the class E PA with finite dc-feed inductance and series inductance.
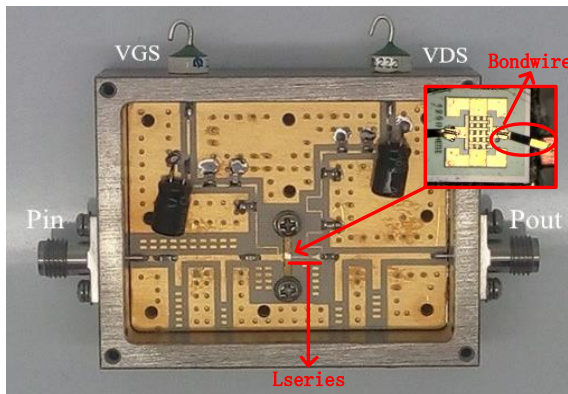

Fig. 11. Photo of fabricated class E PA with finite dc-feed inductance and series inductance.

Figure 12 shows the measured drain efficiency (DE), power added efficiency (PAE), output power, and gain at input power (CW) at 3.1 GHz. The maximum PAE is 63.4% when the input power is 28 dBm.

Figure 13 shows the measured behavior of DE, PAE [25], output power, and output power gain at the input power of 27 dBm. It can be seen that, the output power gain is large than 8.2 dB, while the output power is more than 35.2 dBm between 2.5 GHz and 3.5 GHz (33.3% fractional band width (FBW)).

Figure 14 shows the simulated and the measured power second harmonic over the bandwidth. The maximum power of second harmonic in this frequency band is -22 dBc at 2.5 GHz and the minimum is -55 dBc at 3.0 GHz. Most of the second harmonics power is below
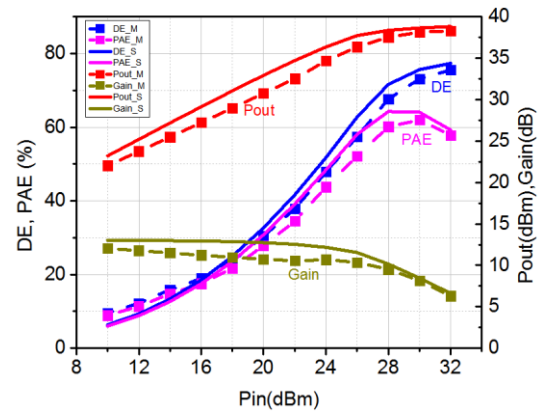
-30 dBc.

Fig. 12. Simulated and measured DE, PAE, output power and gain versus input power at 3.1 GHz continuous input signal.
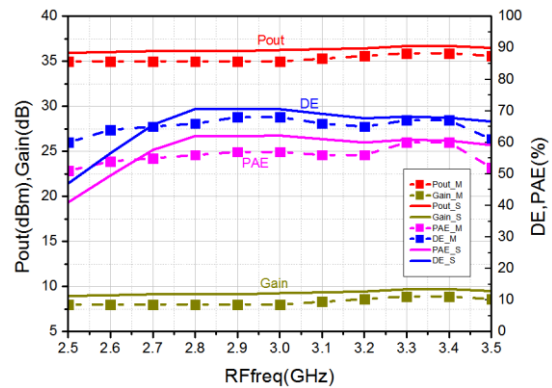

Fig. 13. Simulated and measured frequency dependence of DE, PAE, and Gain characteristics performance.
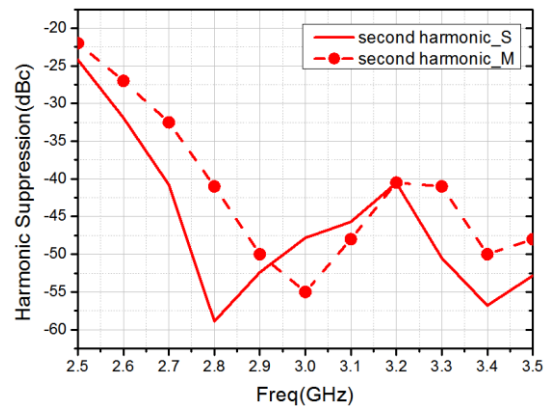

Fig. 14. Simulated and measured second harmonic power.

The measured performance of the proposed PA is compared with other state-of-the-art class E Pas. The results show that the proposed PA can achieve more than

60% DE in such high frequency as summarized in Table 2. The amplifier shows competitive drain efficiency and bandwidth in higher operation frequency. Because of the small gate-width device applied in the present PA, the output power is not very large. However, this report has the highest operation frequency. We can acquire higher output power through increasing the gate-width.

Table 2: Comparison of state of the art GaN PAs

	(GHz)/FBW (%)	DE (%)	Pout
2010 [21]	1.9-2.9 (42%)	>63	45.8 dBm
2011 [22]	2.15-2.5 (15%)	>60	>23 dBm
2011 [23]	0.9-2.2 (84%)	>63	>10 W
2014 [24]	2.52-2.64 (4.6%)	>60	>39 dBm
2015 [25]	1.7-2.8 (48.8%)	>60.3	>19.5 W
2016 [15]	1.4-2.7 (63.4%)	>63	>39.7 dBm
This work	2.5-3.5 (33.3%)	>60	>35.2 dBm

V. CONCLUSION

The class E power amplifier with finite dc-feed inductance and series inductance is analyzed in time domain. Analytical expressions of optimum parameters of the load network are derived. It suggests that the topology can be used in higher operation frequency and broadband PA design with competitive efficiency. A GaN HEMT class E PA with finite dc-feed inductance and series inductance is fabricated and measured. The experimental data and theoretical predictions are found in good agreements. The proposed structure may be useful in the coming 5G communication systems.

REFERENCES

[1]   A. Grebennikov, N. O. Sokal, and M. J. Franco, *Switchmode RF and Microwave Power Amplifiers*. New York, NY, USA: Academic, 2012.

[2]   R. Zulinski and J. Steadman, "Class E power amplifiers and frequency multipliers with finite DC-feed inductance," *IEEE Transactions on Circuits and Systems*, vol. 34, no. 9, pp. 1074-1087, Sep. 1987.

[3]   M. Acar, A. J. Annema, and B. Nauta, "Generalized design equations for class-E power amplifiers with finite DC feed inductance," *2006 European Microwave Conference, Manchester*, pp. 1308-1311, 2006.

[4]   D. Milosevic, J. van der Tang, and A. Van Roermund, "Explicit design equations for class-E power amplifiers with small DC-feed inductance,"

Circuit Theory and Design, 2005. Proceedings of the 2005 European Conference on IEEE, 2005: III/101-III/104, vol. 3, 2005.

[5]   C. P. Avratoglou, N. C. Voulgaris, and F. I. Ioannidou, "Analysis and design of a generalized class E tuned power amplifier," *IEEE Transactions on Circuits and Systems*, vol. 36, no. 8, pp. 1068-1079, Aug. 1989.

[6]   C. H. Li and Y. O. Yam, "Maximum frequency and optimum performance of class E power amplifiers," IEEE *Proceedings - Circuits, Devices and Systems*, vol. 141, no. 3, pp. 174-184, June 1994.

[7]   M. Acar, A. J. Annema, and B. Nauta, "Analytical design equations for class-E power amplifiers," *IEEE Transactions on Circuits and Systems I: Regular Papers*, vol. 54, no. 12, pp. 2706-2717, Dec. 2007.

[8]   J. Y. Hasani and M. Kamarei, "Analysis and optimum design of a class E RF power amplifier," *IEEE Transactions on Circuits and Systems I: Regular Papers*, vol. 55, no. 6, pp. 1759-1768, July 2008.

[9]   M. D. Wei, D. Kalim, D. Erguvan, S. F. Chang, and R. Negra, "Investigation of wideband load transformation networks for class-E switching-mode power amplifiers," *IEEE Transactions on Microwave Theory and Techniques*, vol. 60, no. 6, pp. 1916-1927, June 2012.

[10] A. F. Jaimes and F. R. de Sousa, "Simple expression for estimating the switch peak voltage on the class-E amplifier with finite DC-feed inductance," *2016 IEEE 7th Latin American Symposium on Circuits & Systems (LASCAS)*, Florianopolis, pp. 183-186, 2016.

[11] C. Wang, et al., "An electrothermal model for empirical large-signal modeling of AlGaN/GaN HEMTs including self-heating and ambient temperature effects," *IEEE Transactions on Microwave Theory and Techniques*, vol. 62, no. 12, pp. 2878-2887, Dec. 2014.

[12] Z. Wen, Y. Xu, C. Wang, et al., "An efficient parameter extraction method for GaN HEMT small-signal equivalent circuit model," *International Journal of Numerical Modelling Electronic Networks Devices & Fields*, 2015.

[13] A. Grebennikov, "Load network design techniques for class E RF and microwave amplifiers," *High Frequency Electronics*, vol. 3, no. 7, pp. 18-32, 2004.

[14] A. Grebennikov, "Load network design technique for switched-mode tuned class E power amplifiers," *High Frequency Electron*, vol. 3, no. 7, pp. 1-23, 2004.

[15] A. Grebennikov, "High-efficiency class-E power amplifier with shunt capacitance and shunt filter," *IEEE Transactions on Circuits and Systems I:*

Regular Papers, vol. 63, no. 1, pp. 12-22, Jan. 2016.

[16] Y. Xu, C. Wang, H. Sun, et al., "A scalable large-signal multiharmonic model of AlGaN/GaN HEMTs and its application in C-band high power amplifier MMIC," *IEEE Transactions on Microwave Theory and Techniques*, vol. PP, no. 99, pp. 1-11, 2017.

[17] V. Zomorrodian, U. K. Mishra, and R. A. York, "Modeling of CPW based passive networks using Sonnet simulations for high efficiency power amplifier MMIC design," *Applied Computational Electromagnetics Society Journal*, vol. 26, no. 2, pp. 131-140, 2011.

[18] O. Kizilbey, O. Palamutçuogullari, S. B. Yarman, "3.5-3.8 GHz class-E balanced GaN HEMT power amplifier with 20W Pout and 80% PAE," *IEICE Electronics Express*, vol. 10, no. 5, pp. 20130104-20130104, 2013.

[19] S. Hietakangas and T. Rahkonen, "Input impedance of class E switching amplifiers," *2011 Workshop on Integrated Nonlinear Microwave and Millimetre-Wave Circuits*, Vienna, pp. 1-4, 2011. doi: 10.1109/INMMIC.2011.5773341

[20] V. P. Mcginn and V. A. Demir, "Dynamic measurement method for determining the output impedance of an RF power amplifier," *Applied Computational Electromagnetics Society Journal*, vol. 27, no. 4, pp. 302-310, 2012.

[21] D. Y. T. Wu, F. Mkadem, and S. Boumaiza, "Design of a broadband and highly efficient 45W GaN power amplifier via simplified real frequency technique," *Microwave Symposium Digest (MTT), 2010 IEEE MTT-S International*, Anaheim, CA, pp. 1090-1093, 2010.

[22] M. Thian, V. Fusco, and P. Gardner, "Power-combining class-E amplifier with finite choke," *Circuits & Systems I Regular Papers IEEE Transactions on*, vol. 58, no. 3, pp. 451-457, 2011.

[23] K. Chen and D. Peroulis, "Design of highly efficient broadband class-E power amplifier using synthesized low-pass matching networks," *IEEE Transactions on Microwave Theory and Techniques*, vol. 59, no. 12, pp. 3162-3173, Dec. 2011.

[24] X. Du, J. Nan, W. Chen, and Z. Shao, "'New' solutions of Class-E power amplifier with finite dc feed inductor at any duty ratio," *IET Circuits, Devices & Systems*, vol. 8, no. 4, pp. 311-321, July 2014.

[25] Y. Sun and X. Zhu, "Broadband continuous class-F^{-1} amplifier with modified harmonic-controlled network for advanced long term evolution application," *IEEE Microwave and Wireless Components Letters*, vol. 25, no. 4, pp. 250-252, Apr. 2015.

Chuicai Rong received the Bachelor of Science in Physics from Liaocheng University, Liaocheng, China, in 2000. Master of Science in Theoretical Physics from Qufu Normal University, Qufu, China, in 2006, and is currently working toward the Ph.D. degree at University of Electronic Science and Technology of China (UESTC). His research interests include microwave PA design and RF integrated circuit (RFIC) design.

Xiansuo Liu was born in Anhui Province, China, in 1992. He received the B.S. degree in University of Electronic Science and Technology of China (UESTC), Chengdu, China, in 2015, and is currently working toward the M.S. degree in Electromagnetic Field and Microwave Techniques from the UESTC. His current research interests include wideband high efficiency power amplifier and MMIC.

Yuehang Xu (M'11) was born in Zhejiang Province, China, in 1981. He received the B.S. and M.S. degree in Electromagnetic Field and Microwave Techniques from University of Electronic Science and Technology of China (UESTC), Chengdu, China, in 2004 and 2007, respectively, and the Ph.D. degree from the UESTC joined with Columbia University New York, NY, USA, in 2010.

He joined the Department of Electronic Engineering, UESTC, in December 2010 and was promoted to Associate Professor in August 2012. He is an author or a co-author of more than 30 scientific papers in international journals and conference proceedings. His current research interests are on modeling and characterization of micro/nano-scale electronic devices for radio frequency applications, especially on GaN HEMTs and graphene electronics.